Convergent Use of $\pi-\pi$ Interactions and Iron(II) Coordination in the Binding of Nitriles and Other Substrates to a Conformationally Flexible Macrocyclic Receptor, $Fe(dmgBPh_2)_2$[1]

Dennis V. Stynes

Department of Chemistry, York University, North York, Ontario, Canada M3J1P3

Received December 8, 1993[⊗]

A versatile flexible host is described which makes convergent use of coordinate covalent binding and $\pi-\pi$ interactions. Facile conversion between C_{2h} and C_{2v} conformations of bis((dimethylglyoximato)diphenylborato)-iron (II) complexes, $Fe(dmgBPh_2)_2$, moves boron-linked phenyl groups into or out of intimate contact with iron-bound axial ligands. The $\pi-\pi$ interactions between bound substrates and peripheral phenyl groups span some 8 kcal/mol in energy from repulsive (2-methylimidazole, pyridine, benzonitrile, 2-cyanopyridine, 9-cyanoanthracene) to attractive (phthalonitriles, nitrobenzonitriles, 2- and 4-cyano-*N*-methylpyridinium ion, methylpyrazinium ion, dichlorodicyanobenzoquinone, tetracyanoethylene). Both attractive (charge transfer) and repulsive $\pi-\pi$ interactions are dominated by Coulombic forces. They add to or subtract from the stronger metal−ligand bonding interaction, producing net effects of 10^6 on substrate-binding equilibria and dissociation rates. The convergent dynamic use of several weak interactions is demonstrated via the controlled manipulation of fragment positioning with this molecular device.

Introduction

The positioning of molecular fragments within a structure so as to exploit repulsive or attractive forces between nonbonded atoms is a familiar strategy in chemistry. This approach is especially important in studies of ligand binding to superstructured metalloporphyrins[2] and in host−guest systems.[3]

In superstructured metalloporphryins, repulsive interactions at crowded binding sites can produce dramatic reductions in binding constants.[2a−h] In a few cases, somewhat enhanced binding inside vs outside larger cavities has been attributed to attractive nonbonded contacts between the ligand and the superstructure.[2d,i,j] The presence of polar fragments within the superstructure has sometimes produced enhanced binding of dioxygen.[2k−m] Substrate contacts with the superstructure have also been used to mimic the regio- and stereospecific reactions of metalloproteins.[2n−p] Systems that achieve precise organization of fragment positions within the superstructure for specific interactions are rare.[2q−s]

Host−guest studies,[3] on the other hand, rely on exquisite preorganization to produce non-covalent binding of small guests by synthetic hosts. These studies necessarily make use of a higher level of complementarity between host and guest than has usually been the case in superstructured metalloporphyrin studies. Rigid host structures have been used to control the position and orientation of fragments for multiple-site recognition of specific guests. The rigidity which is typically designed into most synthetic hosts stands in stark contrast to the conformational flexibility of the proteins which they mimic. The convergent use, by enzymes and proteins, of a multitude of relatively weak electrostatic, coordinate covalent, H-bonding, polar, apolar, and solvation forces relies on this mobility.

The control of weak interactions seems best achieved within a flexible structure possessing a limited number of well-defined conformations.[4] Additional advantages accrue if the host binds a variety of substrate types, permits the control of spatial relationships between the substrate and molecular fragments in the host, and allows for a variation in these fragments **without significantly altering other attributes of the system.**

⊗ Abstract published in *Advance ACS Abstracts,* October 1, 1994.

(1) Abbreviations: $dmgBPh_2^-$, (dimethylglyoximato)diphenylborate; $dmgBF_2^-$, (dimethylglyoximato)difluoroborate; py, pyridine; 2-MeIm, 2-methylimidazole; PhCN, benzonitrile; DNB, dinitrobenzonitrile; DDQ, 2,3-dichloro-5,6-dicyano-1,4-benzoquinone; H_2DDQ, 2,3-dichloro-5,6-dicyano-1,4-dihydroxybenzene; $MePz^+$, methylpyrazinium; TCNE, tetracyanoethylene; NPT, 4-nitrophthalonitrile; PT, phthalonitrile; TNFM, (2,4,7-trinitrofluorenylidene)malononitrile; 2-CNpy, 2-cyanopyridine; $2\text{-}CNpyMe^+$, 2-cyanomethylpyridinium; 9-CNanth, 9-cyanoanthracene.

(2) (a) Traylor, T. G.; Tsuchiya, S.; Campbell, D.; Mitchell, M.; Stynes, D. V.; Koga, N. *J. Am. Chem. Soc.* **1985**, *107*, 604−614. (b) Hashimoto, T.; Dyer, R. L.; Crossley, M. J.; Baldwin, J. E.; Basolo, F. B. *J. Am. Chem. Soc.* **1982**, *104*, 2101−2109. (c) Collman, J. P.; Brauman, J. I.; Iverson, B. L.; Sessler, J. L.; Morris, R. M.; Gibson, Q. H. *J. Am. Chem. Soc.* **1983**, *105*, 3052−3064. (d) Collman, J. P.; Brauman, J. I.; Fitzgerald, J. P.; Hampton, P. D.; Naruta, Y.; P.; Sparapany, J. W.; Ibers, J. I. *J. Am. Chem. Soc.* **1988**, *110*, 3477−3486. (e) Traylor, T. G.; Taube, D. J.; Jongeward, K. A.; Magde, D. *J. Am. Chem. Soc.* **1990**, *112*, 6875−6880. (f) Uemori, Y.; Miyakawa, H.; Kyuno, E. *Inorg. Chem.* **1988**, *27*, 377−382. (g) Desbois, A.; Momenteau, M.; Lutz, M. *Inorg. Chem.* **1989**, *28*, 825−834. (h) Lexa, D.; Momenteau, M.; Saveant, J. M.; Xu, F. *J. Am. Chem. Soc.* **1986**, *108*, 6937−6941. (i) Anderson, H. L.; Hunter, C. A.; Meah, M. N.; Sanders, J. K. M. *J. Am. Chem. Soc.* **1990**, *112*, 5780−5789. (j) Imai, H.; Nakagawa, S.; Kyuno, E. *J. Am. Chem. Soc.* **1992**, *114*, 6719−6723. (k) Tsuchiya, T. *Inorg. Chem.* **1985**, *24*, 4450−4452. (l) Suslick, K. S.; Fox, M. *J. Am. Chem. Soc.* **1983**, *105*, 3507−3510. (m) Lopez, M. A.; Kollman, P. A. *J. Am. Chem. Soc.* **1989**, *111*, 6212−6222. (n) Chang, C. K.; Kuo, M. S. *J. Am. Chem. Soc.* **1979**, *101*, 3413−3414. (o) Cook, B. R.; Reinert, T. J.; Suslick, K. S. *J. Am. Chem. Soc.* **1986**, *108*, 7281−7286. (p) Naruta, Y.; Tani, F.; Ishihara, N.; Maruyama, K. *J. Am. Chem. Soc.* **1991**, *113*, 6865−6872. (q) Benson, D. R.; Valentekovich, R.; Diederich, F. *Angew. Chem., Int. Ed. Engl.* **1990**, *29*, 191−193. (r) Lee, C.; Garcia, B.; Bruice, T. C. *J. Am. Chem. Soc.* **1990**, *112*, 6434−6435. (s) Hamilton, A.; Lehn, J.-M.; Sessler, J. L. *J. Am. Chem. Soc.* **1986**, *108*, 5158−5167.

(3) (a) Rebek, R., Jr. *Angew. Chem., Int. Ed. Engl.* **1990**, *102*, 245−255. (b) Diederich, F. *Cyclophanes*; Monographs in Supramolecular Chemistry; Royal Society of Chemistry: Cambridge, U.K., 1991. (c) Sijbesma, R. P.; Wijmenga, S. S.; Nolte, R. J. M. *J. Am. Chem. Soc.* **1992**, *114*, 9807−9813. (d) Cochran, J. E.; Parrot, T. J.; Whitlock, B. J.; Whitlock, H. W., Jr. *J. Am. Chem. Soc.* **1992**, *114*, 2269−2270. (e) Zimmerman, S. C.; Wu, W.; Zeng, Z. *J. Am. Chem. Soc.* **1991**, *113*, 196−201. (f) Hamilton, A. D.; Chang, S.; Van Engen, D.; Fan, E. *J. Am. Chem. Soc.* **1991**, *113*, 7640−7645. (g) Ferguson, S. B.; Sanford, E. M.; Seward, E. M.; Diederich, F. *J. Am. Chem. Soc.* **1991**, *113*, 5410−5419.

(4) (a) Busch, D. H.; Stephenson, N. A. *Coord. Chem. Rev.* **1990**, *100*, 119. (b) Lin, W.; Alcock, N. W.; Busch, D. H. *J. Am. Chem. Soc.* **1991**, *113*, 7603−7608.

0020-1669/94/1333-5022$04.50/0

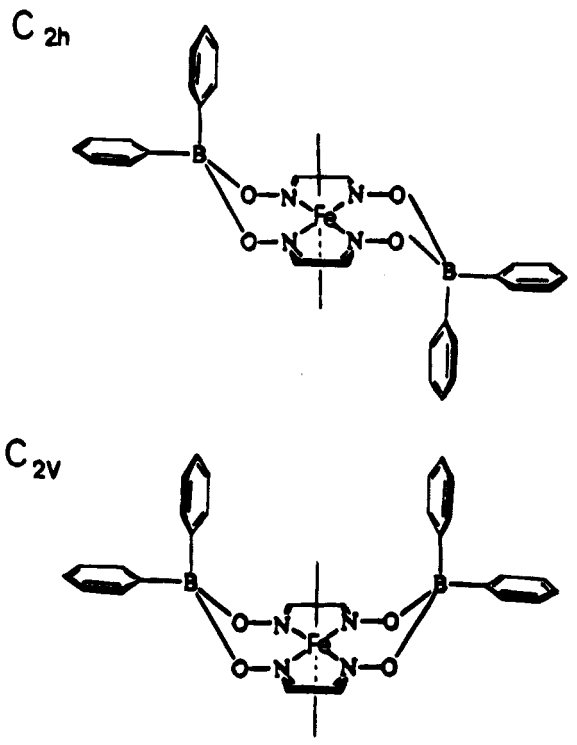

Figure 1. Conformations of $Fe(dmgBPh_2)_2$.

Boron-functionalized vicinal dioxime complexes of Fe(II) meet these criteria.[5] They bind virtually all simple monodentate ligands.[6] The metal−ligand bond (10−30 kcal/mol in $\Delta G^{\ddagger}$) spans the energy regime between covalent bonds (50−100 kcal/mol) and much weaker noncovalent molecular interactions (0−10 kcal/mol). Conformational changes in the macrocycle permit the controlled positioning of boron-linked groups in close proximity to substrate binding sites.[5,7,8] These groups may be varied with minimal changes in structure or metal−ligand interaction.

The binding site enclosed between two parallel phenyl rings in the C_{2v} conformation of $Fe(dmgBPh_2)_2$ (Figure 1) provides an environment similar to those commonly exploited in cyclophanes.[3b-g] The additional metal interaction in this host serves to hold the substrate in position. This extra control permits a more systematic exploration of weaker interactions between more remote regions of the host and substrate. The magnitude of the weak nonbonded interactions (both attractive and repulsive) between molecular fragments may be reliably evaluated in nonaqueous media so as to avoid solvatophobic effects.[3g] While not highly structured or preorganized in the usual sense of these terms, these systems display a variety of extraordinary effects.

In this work, $\pi-\pi$ interactions are explored through the controlled positioning of phenyl groups in face-to-face contact with metal-bound substrates by means of a $Fe(dmgBPh_2)_2$ host. Substrates were rationally selected for a very high degree of geometric complementarity and variable electronic interaction with this host by exploiting the well-established charge transfer interactions of electron-deficient nitriles. Simple amines, on the other hand, provide examples of very poor complementarity with this host.

Experimental Section

Measurements. Proton NMR spectra were recorded on a Bruker AM-300 spectrometer in $CDCl_3$. Electronic spectra were recorded on an Aminco DW2a spectrophotometer (thermostated at 25 °C) and on a Cary 2400 spectrophotometer (near-IR).

Equilibrium constants were obtained by spectrophotometric titrations and analyzed by methods described previously.[6a] Typical conditions of $[FeN_4] = 10^{-4}$ M in 1 cm path length Pyrex cuvettes were used. For $K > 10^4$, a 10 cm path length cell was used with $[FeN_4] = 10^{-5}$ M. Solutions of FeN_4 complexes in CH_2Cl_2 were thermostated at 25 °C. For $MePz^+$, a stock solution of methylpyrazinium iodide in methanol was used owing to its limited solubility in CH_2Cl_2. For 2- and 4-cyanomethylpyridinium iodide,[9b] solubility limitations required the use of 30% methanol/CH_2Cl_2 as solvent.

Kinetic data were obtained by injecting an excess of pyridine (0.1−1.0 M) as entering ligand into solutions of $Fe(dmgBPh_2)_2(py)(RCN)$ in CH_2Cl_2. Least-squares fits of absorbance data gave rate constants independent of wavelength and independent of [py] over this range. In some cases CO, tosylmethyl isocyanide, or tributyl phosphite was also used as the entering group and gave identical rates.

Materials. Dichloromethane was dried over molecular sieves (4 Å). Ligands were commercially available and used as received. $Fe(dmgBF_2)_2(CH_3CN)_2$ and $Fe(dmgBF_2)_2(py)_2$ were prepared as described previously. Analogous BPh_2 derivatives were obtained via reaction of diphenylborinic anhydride[9] with $Fe(dmgH)_2(py)(CO)$. Reaction of the resulting $Fe(dmgBPh_2)_2(py)(CO)$ with pyridine gave $Fe(dmgBPh_2)_2(py)_2$. Three recrystallizations of this product from CH_2Cl_2/CH_3CN afforded $Fe(dmgBPh_2)_2(CH_3CN)_2$. These syntheses will be described in detail elsewhere.[5c]

Results and Discussion

Vicinal dioxime complexes of iron $Fe(diox)_2L_2$ bind a tremendous variety of ligands. Axial ligand substitution reactions proceed via a simple D mechanism.[6] Reactions are followed in nonaqueous solvents by monitoring characteristic metal to oxime (MOxCT) or metal to axial ligand charge transfer (MAxCT) bands, both of which are sensitive to the nature of the axial ligands. Extensive spectral, rate, and equilibrium data have been reported for diox = dmgH and $dmgBF_2$.[6] Gross features of these two systems are retained when the oximate bridging protons are replaced with diphenylboron[7] moieties, BPh_2.

Equilibrium constants for axial ligand substitution reactions (eqs 1 and 2) were obtained by spectrophotometric titration for both BF_2 and BPh_2 systems in CH_2Cl_2 solution. Typical spectral

$$Fe(CH_3CN)_2 + L \overset{K_1}{\rightleftharpoons} Fe(CH_3CN)(L) \overset{K_2}{\rightleftharpoons} FeL_2 \quad (1)$$

$$Fe(py)_2 + L \overset{K_1}{\rightleftharpoons} Fe(py)(L) \overset{K_2}{\rightleftharpoons} FeL_2 \quad (2)$$

data are shown in Figures 2 and 3. Stepwise replacement of CH_3CN by amine ligands, py, and 2-MeIm produced shifts in the MOxCT band of approximately 50 nm per amine ligand. These were typically titrated at fixed $[CH_3CN]$ and variable [amine]. Results are collected in Table 1.

(5) (a) Stynes, D. V.; Leznoff, D. B.; de Silva, D. G. A. H. *Inorg. Chem.* **1993**, *32*, 3989−3990. (b) Impey, G. A.; Stynes, D. V. *J. Am. Chem. Soc.* **1993**, *115*, 7868−7869. (c) Stynes, D. V.; Impey, G. A.; Leznoff, D. B.; de Silva, D. G. A. H. to be submitted for publication.

(6) (a) Chen, X.; Stynes, D. V. *Inorg. Chem.* **1986**, *25*, 1173−1182. (b) Thompson, D. W.; Stynes, D. V. *Inorg. Chem.* **1990**, *29*, 3815−3822. (c) Thompson, D. W.; Stynes, D. V. *Inorg. Chem.* **1991**, *30*, 636−640. (d) de Silva, D. G. A. H.; Thompson, D. W.; Stynes, D. V. *Inorg. Chem.* **1991**, *30*, 4856−4858. (e) Thompson, D. W.; de Silva, D. G. A. H.; Stynes, D. V. *Inorg. Chim. Acta* **1991**, *188*, 139−144.

(7) (a) Verhage, M.; Hoogwater, D. A.; van Bekkum, H.; Reedijk, J. *Recl. Trav. Chim. Pays-Bas* **1982**, *101*, 351−357. (b) Jansen, J. C.; Verhage, M. *Cryst. Struct. Commun.* **1982**, *11*, 305−308.

(8) (a) $Co(dmgBF_2)_2(CH_3OH)_2$ (C_{2h}): Bakac, A.; Brynildson, M. E.; Espenson, J. H. *Inorg. Chem.* **1986**, *25*, 4108−4114. (b) $Co(dmgBF_2)_2(py)^-$ (C_{2v}): Shi, S.; Daniels, L. M.; Espenson, J. H. *Inorg. Chem.* **1991**, *30*, 3407−3410.

(9) Chremos, G. N.; Weidmann, H.; Zimmerman, H. K. *J. Org. Chem.* **1961**, *26*, 1683.

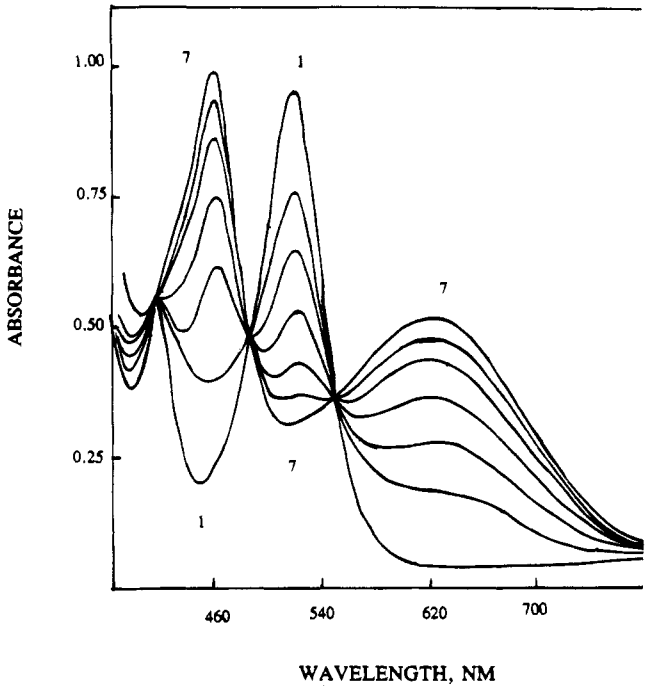

Figure 2. Spectrophotometric titration of $Fe(dmgBPh_2)_2(py)_2$ with 4-nitrophthalonitrile (NPT) in CH_2Cl_2 at [py] = 0.01 M.

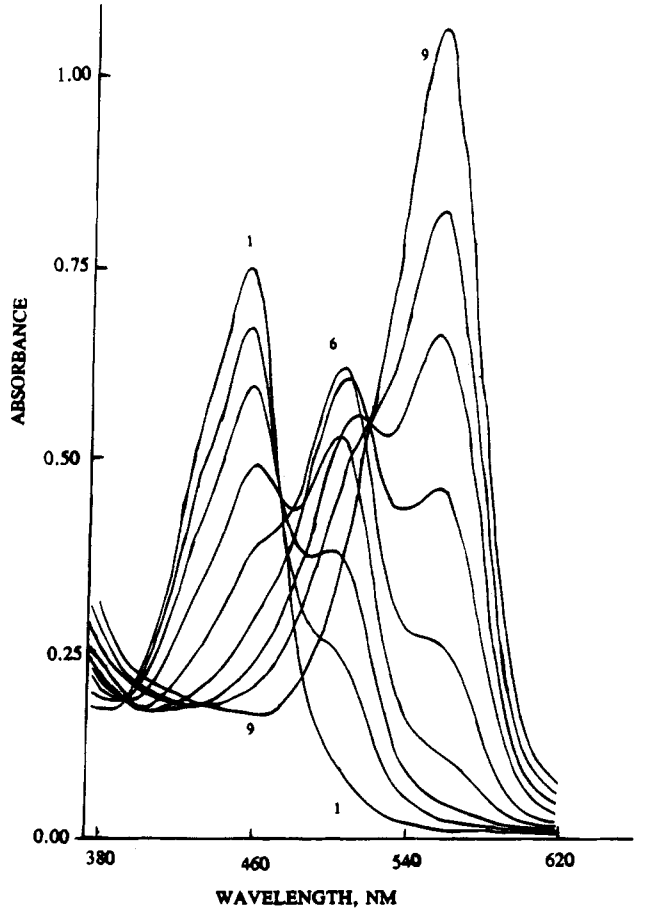

Figure 3. Spectrophotometric titration of $Fe(dmgBPh_2)_2(CH_3CN)_2$ with $BuNH_2$. Conditions: 5.0 M CH_3CN in CH_2Cl_2, [Fe] = 5×10^{-6} M, path length = 10 cm.

Equilibria involving replacement of py in the $FeN_4(py)_2$ complex by amines showed only small shifts in the MOxCT bands, but they gave larger spectral changes in bands assigned to metal to pyridine CT. For $BuNH_2$, distinct spectral changes in the MpyCT bands were observed for each step. For *i*-$PrNH_2$, spectral data for the stepwise replacement of pyridine by amines show a significant overlap in the two steps, making a precise measure of the equilibrium constants difficult. In these cases, we have made use of kinetic data to estimate K_1 and a thermodynamic cycle to obtain K_2.

Table 1.[a] Equilibrium Constants Determined in CH_2Cl_2

	BPh_2			BF_2		
	K_1	K_2	K_1/K_2	K_1	K_2	K_1/K_2
	$FeN_4(CH_3CN)_2 + L \overset{K_1}{\rightleftharpoons} FeN_4(CH_3CN)L \overset{K_2}{\rightleftharpoons} FeN_4L_2$					
$BuNH_2$	4×10^5	5×10^4	8	8×10^5	4.7×10^4	15
i-$PrNH_2$	1×10^4	1.2×10^3	8	2×10^4	1.8×10^3	10
t-$BuNH_2$	25	1.1	22	60	7.1	8
pip	7×10^3	150	50	1.3×10^4	240	54
py[d]	1.2×10^4	4.0	3×10^3	1.8×10^4	250	70
2-MeIm	260	0.1	2.6×10^3	1.6×10^3	10	160
NPT	50	1.0	50			
TCNE[e]	8×10^3	0.55	1.6×10^4	15	6	2
	$FeN_4(py)_2 + L \overset{K_1}{\rightleftharpoons} FeN_4(py)L \overset{K_1}{\rightleftharpoons} FeN_4L_2$					
$BuNH_2$	3.5×10^3	100	35	170[b]	50[c]	3.3
i-$PrNH_2$	15[b]	16[c]	1	3.3[b]	2.4[c]	1.4
PhCN	0.02	3.3×10^{-4}	60	5.9×10^{-3}	1×10^{-4}	59
NPT	22	5×10^{-5} [c]	4×10^5			
TCNE[e]	3×10^4	3×10^{-6} [c]	10^{10}	0.14	1.4×10^{-4} [c]	10^3

[a] Estimated error in K: for $K_1/K_2 > 100$, 10%; for K_1/K_2 between 10 and 100, 15%; for $K_1/K_2 < 10$, 20%. [b] Estimated from kinetic data. [c] Calculated from other equilibria. [d] Reference 5a. [e] Reference 5b.

Rates of dissociation of $BuNH_2$ and *i*-$PrNH_2$ were measured by displacement with pyridine. Two distinct rate processes occur on reaction of $FeN_4(amine)_2$ with pyridine. The faster first step (amine loss trans to amine), $k = 0.016$ s^{-1}, was more conveniently measured using the reaction with isocyanides or other trans delabilizing ligands.[6a] The slower second step (amine loss trans to pyridine) gave rate constants $k_{-BuNH_2} = 0.0038$ and 0.0017 s^{-1} in the BPh_2 and BF_2 systems, respectively. For *i*-$PrNH_2$, the rates in the BF_2 and BPh_2 systems were the same, $k_{-i\text{-}PrNH_2} = 0.08$ s^{-1}. The ratio $k_{+BuNH_2}/k_{+py} = 2.0$ is calculated in the BPh_2 system using K_1 and the reported value[5a] of $k_{-py} = 6.7$ s^{-1}. This ratio is considered reasonable for the more nucleophilic amine ligand. The value of K_1 for the *i*-$PrNH_2$ case was then estimated from kinetic data, and that for K_2 was obtained from a thermodynamic cycle using K_1 and the stepwise constants in Table 1 for *i*-$PrNH_2$ and py ($K_2 = 16 = (10^4)(1.2 \times 10^3)/[(1.2 \times 10^4)(4.0)(15)]$. The calculated values of K_1 and K_2 are nearly the same and agree with crude estimates from titrations. A similar strategy was used for the BF_2 system where $k_{-py} = 0.15$ s^{-1}.[5a]

Nitrile Binding. Equilibrium constants for the binding of nitriles to $Fe(dmgBPh_2)_2(py)_2$ according to eq 3 are collected

$$Fe(dmgBPh_2)_2(py)_2 + RCN \rightleftharpoons Fe(dmgBPh_2)_2(py)(RCN) + py \quad (3)$$

in Table 2. Corresponding values for the BF_2 system, given in parentheses, establish that there is little variation in the metal–nitrile bonding due to electronic effects (as previously found for the $Fe(dmgBF_2)_2(RCN)_2$ complexes[6c]). The largest effect in the BF_2 system is found for TCNE (20-fold greater than that for PhCN of which 4-fold is attributed to a statistical effect in the on-rate constant). The 10^6 variation in K in the BPh_2 system is thus clearly associated with interactions between the nitrile R group and axially directed phenyl groups of the host. These

Table 2. Data[a] for $Fe(dmgBPh_2)_2(py)(RCN)$ Complexes in CH_2Cl_2 at 25 °C

	K			MAxCT	
RCN	BPh_2	BF_2	k_{-RCN}, s^{-1}	nm	cm^{-1}
TCNE[b]	30000	0.14	0.0006	1092	9480
DDQ	2000	0.03	0.007	1552	6445
TNFMN	45		0.20	1023	9780
NPT	22	0.007	0.05 (0 °C)	625	16000
H_2DDQ	5[c]		0.2 (0 °C)	530 sh	18870
PT	3	0.006	5[d]	470 sh	21700
3,5-DNPhCN	0.86			535 sh	18690
3,4-DNPhCN	0.5			600	16667
PhCN	0.02	0.006		406	24630
2-CNpy	0.043	0.0025		423	23641
CH_3CN	0.25	0.004	20[d]		
9-CNanth	0.11	0.008			
$MePz^+$	220	0.11	0.15	770	12990
$2\text{-}CNpyMe^+$	6.3[e]			667	14993
$4\text{-}CNpyMe^+$	3.0[e]			707	14144

[a] Equilibrium constants for the reactions $FeN_4(py)_2 + RCN \rightleftharpoons FeN_4(py)(RCN) + py$. [b] Reference 5b. [c] Estimated from kinetic data by assuming $k_{+RCN}/k_{+py} = 1$ per nitrile group. $k_{-py} = 6.7\ s^{-1}$. [d] Calculated from K with the assumption in footnote *c*. [e] 30% CH_3OH/70% CH_2Cl_2.

interactions range from strongly attractive in the case of TCNE and DDQ to quite repulsive in the case of PhCN and 2-CNpy.

Kinetic data for ligand dissociation was obtained for the more inert nitriles. Limiting rates of RCN dissociation (obtained by reaction with pyridine) are given in Table 2 for the BPh_2 system. For TCNE and DDQ, CO was also used as the entering group and gave identical results. This rules out external charge transfer assistance of ligand loss in these cases. Data for the BPh_2 complexes span over 10^5 in k_{-RCN}. All of the analogous reactions in the BF_2 system are complete on mixing. They are calculated to fall in the range found for CH_3CN when trans to pyridine ($k_{-RCN} = 20\ s^{-1}$) using the relation $K = (k_{-py}/k_{-RCN})(k_{+RCN}/k_{+py})$. The appearance of these effects in the RCN off-rate clearly shows that $\pi-\pi$ interactions with the phenyl groups are lost prior to the transition state for RCN dissociation.

In some cases, equilibria or rates in Table 2 are estimated by assuming reasonable values of the ratio k_{+RCN}/k_{+py}. In all cases where both rate and equilibrium data were obtained, this ratio falls in the range expected on the basis of our extensive study of these systems. Relative rates of addition to the pentacoordinate intermediate may be calculated from $k_{+RCN}/k_{py} = K(k_{-RCN}/k_{-py})$, where $k_{-py} = 6.7\ s^{-1}$. These afford values (TCNE, $3 \times 91 \pm 1$; DDQ, 2 ± 0.5; TNFM, 1.3 ± 0.5) which primarily reflect statistical effects. The peripheral phenyl groups do not discriminate either attractively or repulsively in the addition of ligands of moderate size. Unusual on-rate effects in the BPh_2 system, so far, have only been found in the case of the small diatomic CO ligand.[5a]

The ligands selected in Table 2 possess a low-lying LUMO, and their Fe(II) complexes, like the BF_2 analogues,[6c] display low-energy MAxCT bands. The energy of this electronic transition is roughly correlated with the ligand reduction potential. The methylpyrazinium ion, which gives a MAxCT band at 770 nm, is also included in Table 2. The very good acceptors TCNE and DDQ were selected because of their well-known formation of charge transfer complexes with benzenes.[10-14] Their MAxCT bands are found deep in the near-IR, occurring at 1092 nm for TCNE and 1552 nm for the DDQ complex.

For TCNE and DDQ complexes, additional bands (not found for the BF_2 complexes) in the visible spectra are observed at 504 and 560 nm, respectively. These broader, weaker bands are assigned to through-space phenyl−TCNE[5b] and phenyl−DDQ CT transitions. They provide evidence of the direct interaction between the axial phenyls and the bound nitrile. For comparison, CT bands for the hexamethylbenzene (HMB) complexes of TCNE and DDQ occur at 545 and 581 nm (benzene: 384 and 427 nm, respectively). Analogous transitions are also likely present for some of the other nitriles listed in Table 2, but these bands are typically much broader and weaker than MOxCT bands and occur at higher energies where they are obscured by other features.

We note that the binding of the strong oxidant DDQ[13] without formation of the more common[15] M^+-DDQ^- is made possible by the unusually negative oxidation potential of Fe(II) in these borylated dioxime complexes.[6b] In its semiquinone form, DDQ^- may be expected to have a repulsive interaction with the phenyl groups, making this interaction potentially redox switchable.[16] The bound DDQ in $Fe(dmgBPh_2)_2(py)(DDQ)$ is reduced cleanly to $Fe(dmgBPh_2)_2(py)(H_2DDQ)$ by hydroquinone (H_2Q) with the loss of the 1550 and 550 nm bands and the appearance of a new MAxCT band at 530 nm.

$$Fe(dmgBPh_2)_2(py)(DDQ) + H_2Q \rightarrow Fe(dmgBPh_2)_2(py)(H_2DDQ) + Q \quad (4)$$

In its fully reduced form, H_2DDQ displays a much weaker binding, giving a K_L like that of phthalonitrile.

Conformation. Two conformational isomers of the borylated dioxime macrocycles arise based on axial vs equatorial orientations of the R groups on each boron (Figure 1).[5a] Axially oriented phenyl groups in $Fe(dmgBPh_2)_2$ complexes project over the metal binding site placing them in intimate contact with metal-bound ligands.

In solution, the predominant conformers for $Fe(dmgBPh_2)_2$ complexes are established on the basis of the large upfield shifts of ligand proton resonances when that ligand lies over the face of an axially directed phenyl group and/or by parallel effects of aromatic ligands on BPh_2 resonances. Chemical shift data are collected in Table 3, and conformational assignments are shown in Figure 4. NMR shift mapping[17] and MM2 molecular modeling both place ligand protons within van der Waals contact (3.5 Å) with the face of the axial phenyl groups. Bis-ligated complexes adopt the C_{2h} conformation. When the axial ligands differ, the complex can adopt the C_{2v} conformation in order to minimize repulsive interactions and/or maximize attractive interactions between axial ligands and phenyl groups.

The largest ring-current shifts are experienced when ligands are sandwiched between two phenyl rings. The shifts in these sandwiched ligands are comparable to those reported for inside-bound pyridine protons in picnic basket porphyrins[2d] and for substrate protons lying within the multibenzenoid cavity of a cyclic resorcinol tetramer[18] or other tetrabenzenoid hosts.[3g]

(10) Merrifield, R. C.; Phillips, W. D. *J. Am. Chem. Soc.* **1958**, *80*, 2778−2782.
(11) Liptay, W.; Rehm, T.; Wehning, D.; Schanne, L.; Baumann, W.; Lang, W. *Z. Naturforsch.* **1982**, *37A*, 1427−1448. In kcal/mol units and a 1 M reference state, the stepwise thermodynamic quantities for hmb−TCNE are as follows: $K_1 = 150\ M^{-1}$, ΔG, ΔH, $\Delta S = -2.97, -7.87, -16.4$; $K_2 = 4.9\ M^{-1}$, ΔG, ΔH, $\Delta S = -0.94, -10.79, -33$.
(12) Walker, D.; Hiebert, J. D. *Chem. Rev.* **1967**, *67*, 153−195.
(13) Hammond, P. R. *J. Chem. Soc.* **1963**, 3113−3118.
(14) Prasad, J. *Spectrochim. Acta* **1966**, *A22*, 1869−1875.
(15) Pradella, F.; Scuponi, M.; Sostero, S. *J. Organomet. Chem.* **1991**, *412*, 137−142.
(16) Bernardo, A. R.; Stoddart, J. F.; Kaifer, A. E. *J. Am. Chem. Soc.* **1992**, *114*, 10624−10631.
(17) Bovey, F. A. *Nuclear Magnetic Resonance Spectroscopy*; Academic Press: New York, 1965; p 65.
(18) Kobayashi, K.; Asakawa, Y.; Kikuchi, Y.; Toi, H.; Aoyama, Y. *J. Am. Chem. Soc.* **1993**, *115*, 2648−2654.

Table 3. NMR Data for $Fe(dmgBPh_2)_2LT$ Complexes

L	T	dmg CH_3	BPh_2 A, B, C[a]	ligand resonances α, β, γ[b]	CH_3[c]
$BuNH_2$	$BuNH_2$	[d]2.81	7.37, 7.16, 7.07	1.17, 0.25, 0.74 −0.64 (NH)	0.65
MeIm	MeIm[e]	2.76	7.18, 6.89, 6.84	5.81, 5.96, 6.12	3.09
MeIm	CO[e]	2.42	7.57, 7.21, 7.12 7.23, 7.05, 6.96		3.66
CH_3CN	CH_3CN[f]	2.78	7.45, 7.11, 6.95		1.26
CH_3CN	CO[f]	2.57	7.45, 7.19, 7.1		1.42
CH_3CN	TCNE[g]	2.75	7.51, 7.23, 7.1 7.27, 7.06, 6.95		2.03
CH_3CN	$PMePh_2$	[f]2.31	7.72, 7.45, 7.26 7.25, 7.15, 6.94		0.28 1.60
py	py[f]	2.78	7.17, 6.83, 6.8	7.59, 6.36, 7.15	
py	CO[f]	2.44	7.66, 7.25, 7.2 7.25, 7.0, 7.0	9.02, 6.96, 7.65	
py	CH_3CN[f]	2.69	7.65, 7.35, 7.2 7.24, 7.0, 7.0	8.60, 6.79, 7.65	0.26
py	TCNE[g]	2.63[h] 2.60	7.55, 7.28, 7.2 7.28, 7.08, 7.06	8.78, 6.97, 7.68	
py	DDQ	2.68	7.52, 7.26, 7.2 7.26, 6.80, 6.49	8.72, ..., ...	
py	NPT	2.72[h] 2.70	7.63, 7.33, 7.14 7.25, 6.54, 5.75	8.78, 7.07, 7.48 (py) 8.63, 8.50, 7.95 (NPT)	
py	3,5-DNB	2.76	7.61, 7.31, 7.14 7.25, 6.58, 5.84	8.72, 7.06, 7.52 (py) 9.25, 8.79 (DNB)	
py	$MePh_2P$[f]	2.36	7.66, 7.36, 7.2 6.66, 6.38, 6.4	..., 5.85, ...	1.62

[a] BPh_2, protons, AA′BB′C pattern. Where one set is given, it corresponds to the dynamic average of axial and equatorial environments. Where two are given, the first set is assigned to equatorial phenyls. The assignments of B_{eq} and A_{ax} protons may be reversed in cases where they occur at similar chemical shifts. [b] For py or $BuNH_2$. Other ligand resonances are given below. [c] The methyl resonance of CH_3CN, $BuNH_2$, or $MePPh_2$ is listed. [d] Corresponding assignments for the BF_2 analogue: 2.72 (dmg); −0.14 (NH); 1.45, 1.0, 1.0 (CH_2); 0.72 (CH_3). [e] Reference 7a. [f] Reference 5a. [g] Reference 5b. [h] A splitting of the dmg methyl resonance is observed in these cases.

The aromatic proton resonances of the BPh_2 groups are also indicative of conformation. A single AA′BB′C pattern is found in bis complexes as a result of rapid ring-flips which average equatorial and axial environments. (Averaging of environments because of ligand exchange processes is ruled out by the slow substitution kinetics.) In mixed complexes two different AA′BB′C patterns are found. When phenyls are constrained to face a pyridine, one set of A, B, and C protons is shifted upfield. When benzonitriles are sandwiched, the shift seen for the C proton is at least twice as large as that for the B protons, while the A protons are unshifted. This is consistent with the expected geometry in which the C proton lies over the center of the benzonitrile ring, the B protons lie over an edge, and the A protons lie in a region of low anisotropy above the nitrile group (see Figure 5).

The average magnetic environment of protons in the bound $BuNH_2$ ligand in $Fe(dmgBPh_2)_2(BuNH_2)_2$ is shown by the upfield shifts (relative to the BF_2 analogue) of 0.50, 0.28, 0.75, 0.26, and 0.07 ppm for NH_2, α, β, γ, and δ protons, respectively. The greatest shift is observed for the β protons. The pattern of shifts is definitive evidence for the predominance of the structure shown in Figure 6, which places the average position of the β protons about 4 Å above the center of an axial phenyl ring. The NH protons are in closer contact with the ring (we estimate 2.8 ± 0.2 Å) but lie over an edge where ring-current effects are smaller.

Conformational Effects and Ligand Binding. Conformation and axial ligation are energetically linked in these systems.[5a] Repulsive interactions between bound ligands and axial phenyl groups are relievable by a conformational flip. These effects are clearly seen in the ratio of stepwise formation constants, K_1/K_2, given in Table 1. This ratio is a reliable indicator of ligand-induced conformational flips in the BPh_2 system when trans effects are factored out via comparison with the analogous BF_2 system.

The planar heterocycles pyridine and 2-MeIm, which experience multiple atom−atom contacts in a face-to-face encounter with an axial phenyl, are able to take full advantage of this flip by moving both axial phenyl groups to the open face in a C_{2v} conformer. The ratios of stepwise binding constants for pyridine are 3000 for BPh_2 and 70 for BF_2. Repulsive phenyl−pyridine contacts are introduced only in K_2.

Stepwise displacement of pyridine by nitriles (eq 5) results in dramatically different scenarios for RCN = CH_3CN, PhCN,

$$FeN_4(py)_2 \overset{K_1}{\rightleftharpoons} FeN_4(RCN)(py) \overset{K_2}{\rightleftharpoons} FeN_4(RCN)_2 \quad (5)$$

NPT, and TCNE. The ratios K_1/K_2 are 3000 (CH_3CN), 60 (PhCN), 4×10^5 (NPT), and 10^{10} (TCNE). Benzonitrile experiences a repulsive interaction with axial phenyls comparable in magnitude to that found for pyridine. Therefore, unlike the case with CH_3CN, little relief of face-to-face contacts is possible. When phenyl−RCN contacts are attractive, as in the NPT case, the ratio K_1/K_2 becomes even larger. This implies that both axial phenyls are flipped to interact with NPT. The effects seen in the equilibria are fully consistent with conformational inferences made on the basis of the NMR data.

The enhanced binding of TCNE and NPT, compared to CH_3CN, in eq 6, shows all of the effect in the first step (K_1).

$$Fe(CH_3CN)_2 + RCN \overset{K_1}{\rightleftharpoons} Fe(CH_3CN)(RCN) \overset{K_2}{\rightleftharpoons} Fe(RCN)_2 \quad (6)$$

The values of K_2 are relatively unremarkable. In the sandwiched geometry for $Fe(CH_3CN)$(TCNE) and $Fe(CH_3CN)$(NPT) two TCNE−phenyl/ NPT−phenyl contacts are present. This is the same number that would be present in a C_{2h} conformer of $Fe(RCN)_2$. The system is able to make full use of axial phenyl interactions via conformational flips.

While 1:1 donor−acceptor complexes are better known than 2:1 DAD complexes, this is a consequence of entropic factors. Liptay has found in the hexamethylbenzene−TCNE system that the DAD species has an enthalpy more than twice that of DA.[12] This factor plus the possibly closer π−π contacts and more favorable iron interaction with a trans ligand in a C_{2v} structure explains why we fail to see additional stabilization in the bis species.

Amine Binding. Simple amines bind to $FeN_4(CH_3CN)_2$ in two distinct steps. Unlike the case with pyridine, no unusual differences in the ratio K_1/K_2 or between BF_2 and BPh_2 systems associated with peripheral interactions or conformational flips are evident. This is understood in terms of geometric factors. The primary amine ligands, RNH_2, are seen to favor a C_{2h} conformer with the R group projected away from the axial phenyl. Thus there are no significant contacts with axial phenyls in need of relief. The different geometric demands of amines are also evident in the stepwise constants for replacement of py by amines in Table 1. The large value of the ratio K_1/K_2 for py binding to $Fe(dmgBPh_2)_2(CH_3CN)_2$ is clearly lost. Unlike CH_3CN, primary amines are not readily sandwiched. Repulsive interactions with the amine R group will be introduced if a second axial phenyl is flipped to the amine-bound face.

The proposed orientation of the amine R group away from the axial phenyl in a C_{2h} conformer produces close NH−Ph and NH−F contacts. There is no compelling evidence in the

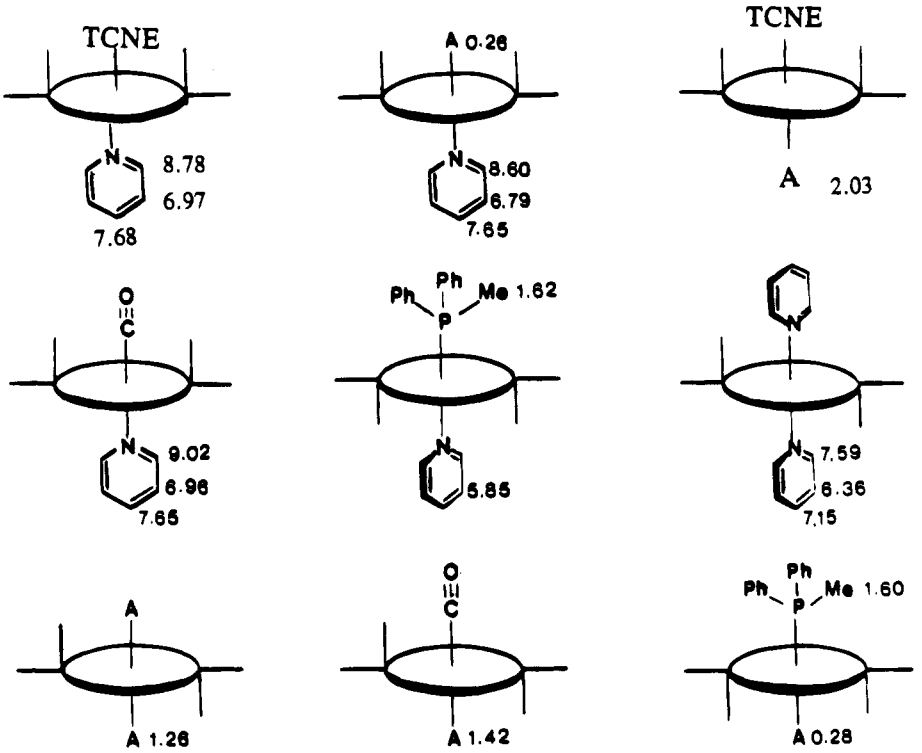

Figure 4. Conformational assignments for $Fe(dmgBPh_2)_2$ Complexes. ^1H NMR shifts for py and methyl protons are given. A = CH_3CN.

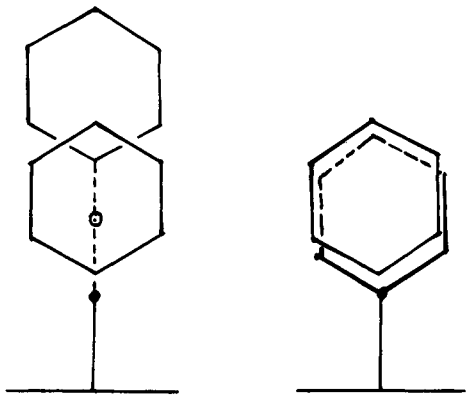

Figure 5. Relative positions of aromatic nitriles (left) and nitrogen heterocycles (right) as viewed through the face of a boron-linked phenyl. An additional phenyl (not shown) lies behind the substrate in "sandwiched" cases.

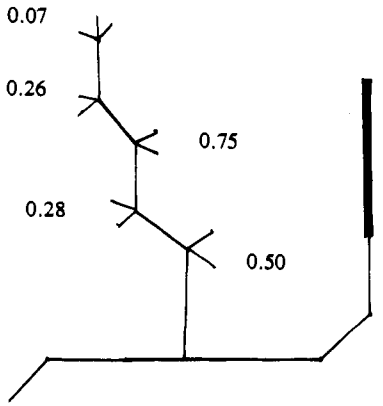

Figure 6. Proposed orientation of $BuNH_2$ in $Fe(dmgBPh_2)_2(BuNH_2)_2$ shown facing a single boron-linked phenyl ring at right. ^1H shifts upfield of the corresponding $Fe(dmgBF_2)_2(BuNH_2)_2$ are given.

equilibrium data of a significant attractive or repulsive interaction which differentiates between the BF_2 and BPh_2 systems. The approximately 2-fold greater K's in the BF_2 system for *n*-$BuNH_2$, *i*-$PrNH_2$, and pip are reasonably assigned to a small electronic effect. The somewhat greater effects evident in the *t*-$BuNH_2$ case are attributed to the greater crowding in the BPh_2 complex. The decline in binding from *n*-$BuNH_2$ to *t*-$BuNH_2$ is consistent with repulsive interactions with atoms in the FeN_4 plane. These effects are significantly greater than those found in the binding to zinc porphyrins,[2j] where such interactions are relieved by movement of the zinc out of the N_4 plane in the pentacoordinate complex.

The CH$-\pi$ interaction has been invoked as a conformation-controlling intramolecular force[19] and more recently as an explanation of small differences between the binding of alcohols to a tetrabenzenoid host[18] and the binding of amines to a bisroof zinc porphyrin.[2j] There is no compelling evidence in our work that CH$-\pi$ interactions contribute significantly energetically. The ^1H resonance shift of the sandwiched CH_3CN is comparable to cases where CH$-\pi$ interactions are invoked, but such shifts are unrelated to energetics. The NH$-\pi$ interaction is expected to be stronger than the CH$-\pi$ interaction owing to the more polar N$-$H bond. Hydrogen bonding to F could also occur in the BF_2 complex. The closest contacts for RNH_2 protons are with the atom directly bound to boron. The CH_3CN protons, in contrast, are well clear of the BF_2 groups.) In order to evaluate the NH$-\pi$ question more fully, we examined the $Fe(dmgBH_2)_2(BuNH_2)_2$ complex[5a] as well as the dmgH system. While primary amines bind better to the BF_2 and BPh_2 systems than to these other systems, the effect is of the order expected on the basis of an electronic effect. Electron-withdrawing groups in the N_4 ligand reduce its donor ability, thus enhancing the binding of strong axial donors.

Quantifying Nonbonded Interactions. Free energies of formation ($-\Delta G$) for complexes in both the BF_2 and BPh_2 systems are collected in Table 4. The values given are obtained via a thermodynamic cycle using the equilibrium constants in Tables 1 and 2 and assigning $\Delta G = 0$ to the parent $Fe(CH_3CN)_2$ complexes. The difference between the two systems $\Delta\Delta G$

(19) Nishio, M.; Hirota, M. *Tetrahedron* **1989**, *45*, 7201–7245.

Table 4.[a,b] $\Delta\Delta G_{298}$ for $Fe(dmgX)_2LT$ in CH_2Cl_2 (kcal/mol)

		$-\Delta G$		
L	T	BF_2	BPh_2	$\Delta\Delta G$
2-MeIm	2-MeIm	5.73	1.95	3.8
py	py	9.07	6.38	2.7
py	PhCN	6.02	4.06	2.0
py	2-CNpy	(6.1)	4.52	1.6
t-$BuNH_2$	*t*-$BuNH_2$	3.6	1.96	1.6
PhCN	PhCN	0.56	−0.68	1.2
CH_3CN	2-MeIm	4.37	3.30	1.1
py	9-CNanth	6.2	5.1	1.1
py	$BuNH_2$	12.1	11.2	0.9
i-$PrNH_2$	*i*-$PrNH_2$	10.30	9.65	0.6
CH_3CN	*t*-$BuNH_2$	2.4	1.90	0.5
CH_3CN	$BuNH_2$	8.05	7.64	0.4
$BuNH_2$	$BuNH_2$	14.46	14.05	0.4
CH_3CN	*i*-$PrNH_2$	5.86	5.45	0.4
CH_3CN	py	5.8	5.56	0.2
py	3,4-DNB	(6.1)	6.0	0.1
CH_3CN	CH_3CN	0	0	0
py	3,5-DNB	(6.1)	6.3	−0.2
py	CO	12.6	12.9	−0.3
py	H_2DDQ	(6.1)	7.3	−0.3
py	PT	6.1	7.0	−0.8
py	2-$CNpyMe^+$	(6.1)	7.47	−1.4
py	$MePz^+$	7.7	9.57	−1.9
py	4-NPT	6.1	8.2	−2.1
TCNE	TCNE	2.7	5.0	−2.3
py	TNFM	(6.1)	8.6	−2.5
CH_3CN	TCNE	1.6	5.3	−3.7
py	DDQ	7.1	10.9	−3.8
py	TCNE	7.9	12.5	−4.6

[a] PhCN = benzonitrile; DNB = dinitrobenzonitrile; PT = phthalonitrile; DDQ = 2,3-dichloro-5,6-dicyano-1,4-benzoquinone; H_2DDQ = 2,3-dichloro-5,6-dicyano-1,4-dihydroxybenzene; TNFM = (2,4,7-trinitrofluorenylidene)malononitrile; $MePz^+$ = methylpyrazinium; TCNE = tetracyanoethylene; 2-CNpy = 2-cyanopyridine; 2-$CNpyMe^+$ = 2-cyanomethylpyridinium; 9-CNanth = 9-cyanoanthracene. [b] Values in parentheses were not measured but are assumed similar to those for PT

$= \Delta G(BF_2) - \Delta G(BPh_2)$ provides a quantitative measure of the sum of all of the "effects" present. A positive value of $\Delta\Delta G$ indicates destabilization of the BPh_2 complex relative to its BF_2 analogue. A negative $\Delta\Delta G$ is indicative of stabilizing interactions in the BPh_2 system not present in the BF_2 analogue. For the most part, $\Delta\Delta G$ measures effects primarily associated with nonbonded contacts between the ligand and boron-linked phenyl groups.

The assignment of a gross thermodynamic difference to a specific local interaction is made with considerable risk in the best of circumstances. The caveat "other things being equal" takes on added significance when effects of a few hundred calories (doubling of a binding constant) are discussed. A 100 cal weak interaction is energetically indistinguishable from a 0.1% change in a single 100 kcal/mol bond or minor adjustments in internal bond angle strain, solvation, etc.! We believe evidence of specific nonbonded interactions in Table 4 is compelling for differences greater than 0.5 kcal/mol but must be viewed cautiously for smaller differences.

The simple amine ligands do not possess adequate geometric complementarity to the superstructure in $Fe(dmgBPh_2)_2$ to permit peripheral effects of a magnitude appropriate for serious discussion. Values of 0.4 kcal/mol for $\Delta\Delta G$ are considered more likely due to a small electronic effect than to peripheral interactions. Even for *t*-$BuNH_2$, where larger effects are found, the effects almost certainly involve a number of structural distortions to relieve contacts with the N_4 plane as well as with peripheral groups. Effects for the 2-MeIm ligand are also complicated by the additional factors associated with contacts with atoms in the N_4 plane.

The much larger effects found for pyridine complexes arise because of geometric factors associated with the interaction of planar fragments. As discussed above, phenyl−py contacts may be relieved by a conformational flip which moves both axial phenyl groups to the opposite face. Thus we observe little difference in $\Delta\Delta G$ values for $FeN_4(py)(CH_3CN)$ and $FeN_4(py)(CO)$. In contrast, $FeN_4(py)_2$ is destabilized in the BPh_2 system by 2.7 kcal/mol as a result of Ph−py contacts in the C_{2h} structure. There are numerous Ph−py atom−atom contacts (Figure 6) in the BPh_2 system but only two F−py atom contacts in the BF_2 system. While contacts with axial fluorines in BF_2 are considered less important, one must remember that $\Delta\Delta G$ measures the difference between F and Ph interactions. In nitrile ligands (RCN) the R group is well clear of the FeN_4 plane and also clear of boron-linked fluorine atoms in the BF_2 system. In addition, there are minimal electronic effects on iron−nitrile binding associated with gross changes in the R group.[6c] Thus they offer a superb opportunity to identify effects associated with peripheral interactions with axial phenyl groups. With the possible exception of the Fe(py)(PhCN) complex, a sandwiched geometry for the nitriles in the Fe(py)(RCN) species is indicated.

The nitriles investigated span the full range of interactions from repulsive to strongly attractive. For nitriles bound trans to pyridine, $\pi-\pi$ stabilization increases in the order PhCN, 2-CNpy, 9-CNanth, 3,4-DNB, CH_3CN, 3,5-DNB, H_2DDQ, PT, 2-$CNpyMe^+$, NPT, TNFM, DDQ, TCNE. Attractive phenyl−substrate contacts occur with the best electron acceptors, especially those known to produce charge transfer complexes with benzenes.

Substrates which experience repulsive interactions with axial phenyl groups are made attractive by the introduction of regions of positive charge density in the substrate. The cationic methylpyrazinium complex, $Fe(py)(MePz^+)$, has a $\Delta\Delta G$ of 4.6 kcal/mol more negative than that of its pyridine analogue, $Fe(py)_2$. This difference is a combination of 2.7 kcal/mol due to relief of Ph−py contacts in a C_{2v} structure and 1.9 kcal/mol of attractive $MePz^+$−Ph interaction. Methylation of 2-CNpy results in a change in $\Delta\Delta G$ from repulsive (1.6 kcal/mol) to attractive (−1.4 kcal/mol). The systematic introduction of polarizing nitro or cyano substituents in PhCN is seen to "tune" $\Delta\Delta G$ from +2.0 kcal/mol in Fe(py)(PhCN) to −2.1 kcal/mol in 4-nitrophthalonitrile. The magnitudes of these effects are truly impressive, considering the fact that no through-bond effects are involved. We attribute this to the exquisite geometric complementarity between the substrate and host and its ability to allow considerable geometric optimization of the interacting fragments, without incurring significant entropic or other energetic losses.

The trends in $\Delta\Delta G$, in cases where planar substrates are sandwiched between phenyl groups, are fully consistent with recent explanations[20] of $\pi-\pi$ interactions. Face-to-face interactions are normally repulsive unless strong polarizing effects are introduced. The charge transfer complexes between a donor such as benzene and good acceptors such as TCNE or DDQ are prime examples of the effects of polarization on the electrostatic contribution to π stacking.[10-14]

Charge transfer transitions arise because of the close proximity of molecular orbitals brought about because of attractive forces between molecular fragments. Since they are a consequence, not a cause,[20] of such interactions, they are not necessarily correlated with the energetics of the interaction. While DDQ displays lower energy MAxCT and Ph−CT bands

(20) (a) Hunter, C. A.; Sanders, J. K. M. *J. Am. Chem. Soc.* **1990**, *112*, 5525−5534. (b) Cozzi, F.; Cinquini, M.; Annuziata, R.; Siegel, J. S. *J. Am. Chem. Soc.* **1993**, *115*, 5330−5331.

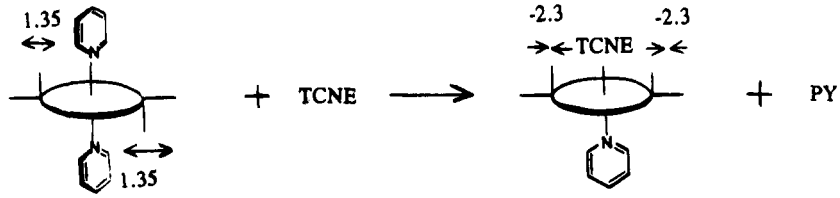

Figure 7. Phenyl–substrate interactions contributing 7.3 kcal/mol in $\Delta\Delta G$ via a conformational flip.

than does TCNE, the magnitude of the $\pi-\pi$ stabilization is greater for TCNE. (Note k_{-RCN} in Table 2 as well as $\Delta\Delta G$ in Table 4.) The charge transfer complexes between benzenes and TCNE are known to be more stable than the analogous DDQ complexes.[14] The terms donor–acceptor and CT interaction are misleading descriptions of what is essentially a Coulombic interaction.[20b] Complementarity is best viewed on the basis of Coulombic factors evident in the match of the substrate's molecular electrostatic potential with regions of negative charge density found on the π faces of phenyl rings.

Electrostatic interactions between regions of complementary charge distribution play an important role in $\pi-\pi$ interactions.[21] Electrostatic effects are also said to contribute to superstructure effects on ligand binding[2m] and protein modulation of heme–CO stretching frequencies.[22]

A cofacial arrangement of planar fragments **amplifies** weak (ca. 100 (cal/mole)/contact) interactions by increasing the area of contact between molecular electrostatic potential surfaces.

The large difference between PhCN and PT was unexpected. However, it is clearly consistent with consideration of electrostatic factors. The electrostatic potential above the ring is less negative for PT than for PhCN, and the partial positive charge on the additional cyano carbon atom in PT lies in close contact with the negative charge density in the phenyl group of the host. This produces a more favorable interaction in the phthalonitrile case. Even larger Coulombic effects obtain in the stronger acceptors NPT, TCNE, and DDQ and the cationic substrates studied.

We have carried out an ab-initio calculation[23] to estimate the electrostatic interaction energy difference between benzo- and phthalonitriles when sandwiched between two benzene rings 3.3 Å apart in a geometry closely approximating that proposed for $Fe(dmgBPh_2)_2(py)(RCN)$ shown in Figure 5. The sandwiched phthalonitrile is found to be 2.2 kcal/mol lower in energy than the sandwiched benzonitrile. The direction and magnitude of the effect are consistent with the measured difference in $\Delta\Delta G$ = 2.8 kcal/mol obtained from Table 4. This simple calculation supports the proposed electrostatic origin of these interactions. Agreement would no doubt improve if we allowed for some geometry optimization (The phenyl group is expected to move toward the free cyano carbon).

An attractive feature of these systems lies in their ability to achieve geometry optimization of $\pi-\pi$ interactions via subtle adjustments in the relative orientation of the planar fragments. This allows positively charged regions of the substrate to improve interactions with negative regions of the phenyl π face.

Dynamic Convergent Use of Multisite Interactions. While most host–guest studies have focused on simple binding energetics, a more important question concerns how convergent use is made of multiple weak interactions, both attractive and repulsive, in a dynamic process. Considerable advantage is obtained by being able to flip interactions on or off. The equilibrium in Figure 7 is illustrative. A 7.3 kcal/mol effect of peripheral nonbonded interactions is found. In this equilibrium, two repulsive 1.35 kcal/mol py–Ph face-to-face interactions are switched off while two attractive TCNE–Ph interactions are switched on. The net effect is twice that which would obtain in a preorganized rigid C_{2h} receptor. Much can be accomplished through manipulations, at the molecular level, in systems of limited flexibility when a high level of control is engineered into the molecular device.[25] Host–guest chemistry can extend beyond elementary considerations of recognition through such devices.

Summary. The following features are demonstrated in this simple molecular device: (1) Planar substrates are positioned in face-to-face contact with one or two phenyl rings. (2) The energetics of phenyl–substrate contacts are quantified on the basis of their additive or subtractive effect on iron–ligand bonds. (3) Nonbonded interactions are turned on or off via the conformational dynamics of the device. (4) Equilibria and rate effects of the order of 10^6 are produced by means of nonbonded interactions. (5) Coulombic effects predominate over donor–acceptor/CT effects even for cases where low-energy phenyl–substrate CT transitions are observed.

Acknowledgment. Preliminary contributions from Dr. D. G. A. H. de Silva, D. B. Leznoff, and G. A. Impey are gratefully acknowledged. I thank Kumud Sharma for running some NMR spectra and York University for financial support.

(21) Hamilton, A. D. *J. Chem. Educ.* **1990**, *67*, 821–828.
(22) Oldfield, E.; Guo, K.; Augsberger, J. D.; Dykstra, C. E. *J. Am. Chem. Soc.* **1991**, *113*, 7537–7541.
(23) Ab-initio calculations were performed at the 3-21G level using the Spartan 2.0 system of programs (Wavefunction Inc., Irvine, CA). Full Cartesian gradient geometry optimization was performed using the constraint cyclization method of Baker.[24] Ring–ring separations were fixed at 3.3 Å for the sandwiched PhCN, and the resulting optimized geometry was not altered for PT. We thank Dr. William Pietro for these calculations.
(24) Baker, J. *J. Comput. Chem.* **1992**, *13*, 240.
(25) Anelli, P. L.; Spencer, N.; Stoddart, J. F. *J. Am. Chem. Soc.* **1991**, *113*, 5131–5133.